



Molecular Dynamics Simulations of Hugoniot Relations for Poly[methyl methacrylate]

**by Tanya L. Chantawansri, Edward F. C. Byrd, Betsy M. Rice,
and Jan W. Andzelm**

ARL-TR-5819

November 2011

NOTICES

Disclaimers

The findings in this report are not to be construed as an official Department of the Army position unless so designated by other authorized documents.

Citation of manufacturer's or trade names does not constitute an official endorsement or approval of the use thereof.

Destroy this report when it is no longer needed. Do not return it to the originator.

Army Research Laboratory

Aberdeen Proving Ground, MD 21005-5066

ARL-TR-5819**November 2011**

Molecular Dynamics Simulations of Hugoniot Relations for Poly[methyl methacrylate]

**Tanya L. Chantawansri, Edward F. C. Byrd, Betsy M. Rice,
and Jan W. Andzelm**

Weapons and Materials Research Directorate, ARL

REPORT DOCUMENTATION PAGE				Form Approved OMB No. 0704-0188	
<p>Public reporting burden for this collection of information is estimated to average 1 hour per response, including the time for reviewing instructions, searching existing data sources, gathering and maintaining the data needed, and completing and reviewing the collection information. Send comments regarding this burden estimate or any other aspect of this collection of information, including suggestions for reducing the burden, to Department of Defense, Washington Headquarters Services, Directorate for Information Operations and Reports (0704-0188), 1215 Jefferson Davis Highway, Suite 1204, Arlington, VA 22202-4302. Respondents should be aware that notwithstanding any other provision of law, no person shall be subject to any penalty for failing to comply with a collection of information if it does not display a currently valid OMB control number.</p> <p>PLEASE DO NOT RETURN YOUR FORM TO THE ABOVE ADDRESS.</p>					
1. REPORT DATE (DD-MM-YYYY) November 2011		2. REPORT TYPE Final		3. DATES COVERED (From - To) 1 October 2010 – 1 October 2011	
4. TITLE AND SUBTITLE Molecular Dynamics Simulations of Hugoniot Relations for Poly[methyl methacrylate]				5a. CONTRACT NUMBER	
				5b. GRANT NUMBER	
				5c. PROGRAM ELEMENT NUMBER	
6. AUTHOR(S) Tanya L. Chantawansri, Edward F. C. Byrd, Betsy M. Rice, and Jan W. Andzelm				5d. PROJECT NUMBER	
				5e. TASK NUMBER	
				5f. WORK UNIT NUMBER	
7. PERFORMING ORGANIZATION NAME(S) AND ADDRESS(ES) U.S. Army Research Laboratory ATTN: RDRL-WMM-G Aberdeen Proving Ground, MD 21005-5066				8. PERFORMING ORGANIZATION REPORT NUMBER ARL-TR-5819	
9. SPONSORING/MONITORING AGENCY NAME(S) AND ADDRESS(ES)				10. SPONSOR/MONITOR'S ACRONYM(S)	
				11. SPONSOR/MONITOR'S REPORT NUMBER(S)	
12. DISTRIBUTION/AVAILABILITY STATEMENT Approved for public release; distribution is unlimited.					
13. SUPPLEMENTARY NOTES					
14. ABSTRACT <p>Using classical molecular dynamics and the polymer-consistent force-field with charges from the condensed-phase optimized molecular potentials for atomic simulation studies force-field, we have calculated Hugoniot curves for the polymer, poly[methyl methacrylate] (PMMA). In this study, the Hugoniot curve was calculated using the Erpenbeck method, where we studied the sensitivity of the calculation on equilibration time, system size, and chain length care. Through this study, we determined that the calculation is relatively insensitive, where short equilibration time, small system sizes, and short chain lengths can be used to obtain shock phase behavior of PMMA.</p>					
15. SUBJECT TERMS polymer, PMMA, Hugoniot					
16. SECURITY CLASSIFICATION OF:			17. LIMITATION OF ABSTRACT UU	18. NUMBER OF PAGES 20	19a. NAME OF RESPONSIBLE PERSON Tanya L. Chantawansri
a. REPORT Unclassified	b. ABSTRACT Unclassified	c. THIS PAGE Unclassified			19b. TELEPHONE NUMBER (Include area code) 410-306-2777

Contents

List of Figures	iv
1. Introduction	1
2. Methodology: Hugoniot Calculation	2
3. Computational Methods	4
4. Results	5
5. Conclusion	12
6. References	13
Distribution List	14

List of Figures

Figure 1. Schematic of Erpenbeck method used to calculate Hugoniot curve.	3
Figure 2. Relative values of the total energy per monomer, density, temperature, and pressure vs. time obtained from NPT simulation for the reference state (~298 K, 1 atm). Relative values were calculated by subtracting the value from the end of the simulation from each data point. Each data point is the average of the last 100 ps.	6
Figure 3. Hugoniot curves for 34 c-100 m-10 ns-0.015 $\mu\text{s/K-0}$ compared to experimental values.	6
Figure 4. Relative values of the total energy per monomer, density, temperature, and pressure vs. time obtained from NPT simulation for the reference state (~298 K, 1 atm). Relative values were calculated by subtracting the value from the end of the simulation from each data point. Each data point is the average of the last 100 ps.	7
Figure 5. Hugoniot curve for 8 c-45 m-10 ns-0.015 $\mu\text{s/K-0}$ and 34 c-100 m-10 ns-0.015 $\mu\text{s/K-0}$	8
Figure 6. Hugoniot curve for 8 c-45 m-2 ns-0.015 $\mu\text{s/K-0}$ and 8 c-45 m-10 ns-0.015 $\mu\text{s/K-0}$	8
Figure 7. Hugoniot curve for 8 c-45 m-100 ps-0.005 $\mu\text{s/K-0}$ and 8 c-45 m-2 ns-0.015 $\mu\text{s/K-0}$	8
Figure 8. Hugoniot curve for 8 c-45 m-100 ps-0.005 $\mu\text{s/K-0}$ and 360 c-1 m-100 ps-0.005 $\mu\text{s/K-0}$	9
Figure 9. Hugoniot curve for 8 c-45 m-100 ps-0.005 $\mu\text{s/K-0}$ and 33 c-4 m-100 ps-0.005 $\mu\text{s/K-0}$	9
Figure 10. Relative values of the total energy per monomer, density, temperature, and pressure vs. time obtained from NVT simulation at elevated pressure and temperature (~1280 K, 28 GPa). Relative values were calculated by subtracting the value from the end of the simulation from each data point. Each data point is the average of the last 100 ps.	10
Figure 11. Relative values of the total energy per monomer, density, temperature, and pressure vs. time obtained from NVT simulation at elevated pressure and temperature (~1300 K, 28 GPa). Relative values were calculated by subtracting the value from the end of the simulation from each data point. Each data point is the average of the last 100 ps.	11
Figure 12. Hugoniot curve for 34 c-100 m-10 ns-0.015 $\mu\text{s/K-10 ns}$ and 34 c-100 m-10 ns-0.015 $\mu\text{s/K-0}$	11
Figure 13. Hugoniot curve for 8 c-45 m-10 ns-0.015 $\mu\text{s/K-10 ns}$ and 8 c-45 m-10 ns-0.015 $\mu\text{s/K-0}$	12

1. Introduction

The behavior of polymers under extreme conditions (high pressure and temperature) is of interest for both civilian and military applications, such as polymer-bonded explosives, coatings, adhesives, and lightweight armor. Insight into the response and energy dissipation mechanisms of such materials to ballistic impact of projectiles is necessary in order to design and develop novel materials to improve the protection of the Future Force. The material properties and response at extreme conditions can be determined through shock experiments, which are often difficult to measure experimentally because of difficulties in traversing a large range of pressures (up to hundreds of gigapascals) and temperatures (thousands of kelvin) with available instrumentation. In addition, interesting behavior, such as observed behind a shock front, occurs at extremely short time and length scales (nanoscale), which poses problems in characterizing the material using current experimental capabilities. To further understand the shocked systems, simulation methods such as molecular dynamics (MD) and quantum mechanics can be used to provide insight into atomic-level phenomena.

The shock response of a material can be described by its shock Hugoniot, which is the locus of thermodynamical states accessible by shock loading from a given thermodynamic initial condition. This calculation can be performed through a variety of methods, such as quantum mechanical theories (wave function-based methods and density functional theory) and classical atomistic simulation methods, such as MD and reactive Monte Carlo. Insight into atomic-level phenomenon of these materials at extreme conditions is most readily extracted using the MD simulation method, where regimes not accessible by experimental techniques can be accessed. MD computation of the Hugoniot state can be obtained through several different types of simulations. One can involve the calculation of properties behind the shock discontinuity in a shock wave simulation (1). Another method introduced by Erpenbeck (2) involves generating an equation of state for the subsequent evaluation of Hugoniot conservation relations (3). An equilibrium uniaxial Hugoniot method can also be employed that uses equations of motion which restrain the system during the simulation so that the time average properties amount to the Hugoniot curve (4).

One of the main limitations of MD is that the accuracy of the results is highly dependent on the description of the forces acting on the particles. An erroneous description can lead to inaccurate results, thus it is important to determine the quality and applicability of the force field that describes the interactions between molecules. Therefore, in order to properly depict the material properties of materials subjected to the extreme temperatures and pressures corresponding to shock conditions, force fields must also be accurate for both the shocked and unshocked states. In addition, during shock experiments, bonds between atoms in the material may break and the formation of new reaction products can occur. This behavior will require the use of a reactive

potential (i.e., one that describes making and breaking of chemical bonds) whose parameterization is currently an area of interest (5). Most reactive potentials available for polymers are highly idealized representations, although ReaxFF is emerging as one that can properly describe chemistry. In lieu of accurate reactive potentials, numerous studies rely on nonreactive potentials that have been extensively parameterized and tested against systems at ambient conditions.

The purpose of this study is to assess the quality of a popular nonreactive interaction potential in describing the shock properties of amorphous atactic poly[methyl methacrylate] (PMMA) through MD simulation. In this study, we use the polymer-consistent force field (PCFF) with condensed-phase optimized molecular potentials for atomic simulation studies (COMPASS) charges. We will investigate the effect of varying system size, equilibration time, and chain length on the calculated Hugoniot curve. We will also consider relatively low pressures (moderate compressed systems) where bond breaking does not occur, which justifies the use of a nonreactive force field.

2. Methodology: Hugoniot Calculation

Although several methods exist to calculate the Hugoniot curve, we evaluated the Hugoniot points through a procedure developed by Erpenbeck (2), which involves performing several constant particle, volume, and temperature (NVT) simulations at multiple temperatures for several compressed structures. The Hugoniot curve consists of the set of pressure-volume-temperature points for which the Hugoniot expression

$$H_g = E - E_o + \frac{1}{2}(P + P_o)(V - V_o) \tag{1}$$

is 0. In this equation, E is the specific internal energy per unit mass (sum of the kinetic and potential energy), P is the pressure, and $V = 1/\rho$ is the specific volume (ρ is the density). The term *specific* refers to the quantity per unit mass, while the subscript “o” refers to the quantity in the initial unshocked state.

The Hugoniot points are calculated through several MD simulations, where a series of NVT simulations are performed over a range of temperatures at a fixed specific volume after the system is annealed and relaxed. To obtain systems at different specific volumes, the polymer is compressed isotropically at a specified pressure and allowed to equilibrate under constant temperature and pressure (NPT) MD simulations ($T = 298$ K). Using the equilibrated structure obtained at the desired pressure, we performed a series of sequential NVT-MD simulations where the temperature was incrementally increased after a prescribed simulation time. After the temperature scan, the Hugoniot function (equation 1) is evaluated at each temperature; this produces a series of equation-of-state points as a function of temperature for each specific volume, which can be interpolated through a linear line to locate the temperature (the Hugoniot temperature) at which the expression is 0. Finally, to obtain the Hugoniot pressure, the

pressure and temperature data are fitted with a linear equation and evaluated at the Hugoniot temperature. Since the linear fit was only performed on the points which bracket the Hugoniot temperature and pressure, the temperature scan ceased once the Hugoniot point was bracketed. Further NVT-MD simulations can be performed to ensure that these two points are at equilibration. For a schematic, see figure 1.

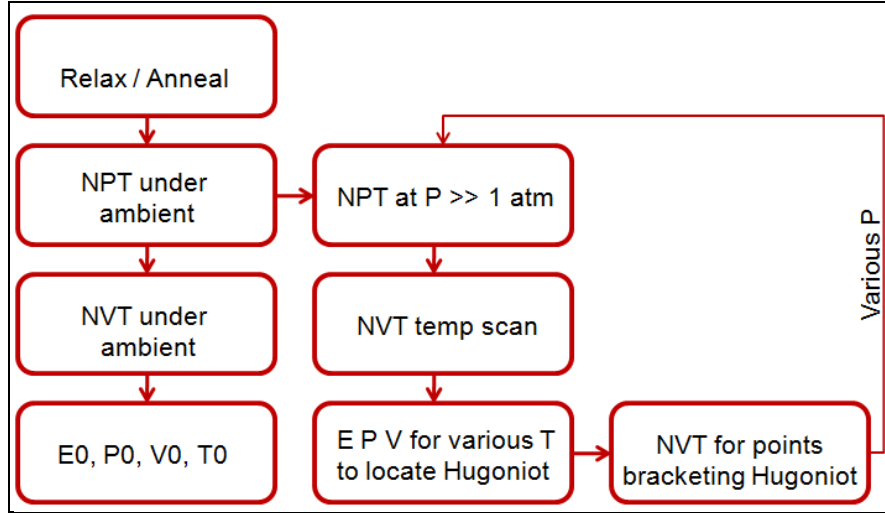


Figure 1. Schematic of Erpenbeck method used to calculate Hugoniot curve.

Experimentalists tend to report shock Hugoniot data in terms of the U_{st} and U_{pt} , which are the shock and particle (or mass) velocities, respectively. To obtain these values from the P and V data points, the following equations can be used:

$$U_{st} = \sqrt{\frac{V_o(P - P_o)}{1 - V/V_o}}, \quad (2)$$

and

$$U_{pt} = \sqrt{V_o(P - P_o)(1 - V/V_o)}. \quad (3)$$

On the same note, the experimental data can be converted into P and V data by rearranging equations 2 and 3:

$$V = \frac{V_o(U_{st} - U_{pt})}{U_{st}}, \quad (4)$$

and

$$P = P_o + \frac{U_{st}U_{pt}}{V_o}. \quad (5)$$

3. Computational Methods

MD simulations were performed using the open-source classical molecular dynamics code large-scale atomic/molecular massively parallel simulator (LAMMPS) (6, 7). We have interfaced amorphous polymer builders with LAMMPS using the commercial visualization package materials processes and simulations (MAPS) (8). MAPS was used to create a periodic cell of PMMA and assign the PCFF force field, where the COMPASS charges were obtained using Materials Studio (9). To produce the three-dimensional periodic cell, we used a well-established method to build the so-called amorphous cells. This method uses a Monte-Carlo technique to build an amorphous structure of the polymer followed by the energy minimization of the bulk structure. The scheme builds polymeric chains by using rotational isomeric state theory and taking into account nonbonded interactions with the already constructed neighboring chains, including their periodic images (10).

PCFF is a class 2 force field where the nonbonded interactions are composed of a 9-6 Lennard Jones potential (van der Waals) and a Coulombic pairwise (electrostatic) interaction. In our simulation, we used a cutoff of 12.0 Å for both interactions. We also included an accurate description of the long-range electrostatic interaction using the particle-particle, particle-mesh method with a precision of $1.0\text{e-}6$.

Temperature and pressure were controlled using the Nose-Hoover thermostat with a 100 fs coupling constant and the Nose-Hoover barostat with 1000 a fs coupling constant, respectively. For the NPT simulations, the three diagonal components were coupled together when the pressure was computed, and the dimensions dilated and contracted in concert. In addition, a time step of 1 fs was used for all simulations unless otherwise noted.

All simulations were initially relaxed and annealed. Relaxing the structure involved energy minimization followed by four stages of NVE (constant, particle, volume, and energy) simulations with velocity rescaling as the thermostat. The energy minimization was performed using the Polak-Ribiere conjugate gradient method with a maximum of 10,000 steps. The energy and force tolerance was set to 0 and $1.0\text{e-}8$, respectively, with a maximum of 10,000,000 evaluations. During the NVE simulations, the time step was increased for each stage: 0.001 to 0.010 to 0.100 to 1.000, where a total of 10,000 time steps was performed for each stage. The velocity-rescaling frequency, window, and fraction were set to one step, 0.01 K and 1.0, respectively. After relaxing the structure, annealing was performed through five cycles, where each cycle was composed of 50 ps of NPT at 298.15 K \rightarrow NPT heating at a rate of 0.67 ps/K to 600 K \rightarrow 50 ps of NPT at 600 K \rightarrow NPT cooling at a rate of 0.1656 ps/K to 298.15 K \rightarrow energy minimization. The energy minimization utilized the same parameters as in the structure relaxation.

We studied the effect of varying equilibration time, system size, and chain size. To differentiate between the different systems, we labeled each one with a descriptor that combined the number of chains in the simulation box, number of monomers per chain, NPT equilibration time for reference state, heating rate of NVT temperature scan, and additional NVT equilibration time for the points that bracket the Hugoniot point. For instance, 34 c-100 m-10 ns-0.015 $\mu\text{s/K}$ -0, indicated a system with 34 chains composed of 100 monomers, where 10 ns of NPT was used to obtain the reference state. The NVT temperature scan was performed using a heating rate of 0.015 $\mu\text{s/K}$, and we did not perform any additional NVT equilibration time for the points that bracket the Hugoniot.

4. Results

Initially, we considered a system composed of 34 chains of atactic PMMA, which are composed of 100 repeat units each (equivalent to one entanglement per chain). This equates to approximately 50,000 atoms. After relaxing and annealing the system, NPT was performed for over 10 ns, where the relative values for the total energy per monomer (n), density, temperature, and pressure vs. time are shown in figure 2. Relative values were calculated by subtracting the value of the end of the simulation time from each data point. From the figure, we clearly observed that the total energy/density continued to decrease/increase with time beyond 10 ns. The difference was quite small $O[0.1]$ for the total energy per n and $O[0.01]$ for density), and the values appeared to be leveling off. It would be interesting, however, to note how equilibration time could affect the shape of the Hugoniot curve.

The Hugoniot curve for 34 c-100 m-10 ns-0.015 $\mu\text{s/K}$ -0 is shown in figure 3, where our simulated curve is compared with experimental data. The MD results agreed well with experiment for low-to-moderate pressures (up to ~ 20 GPa), where deviations were observed at higher pressures.

To determine if a smaller system would be able to reproduce the Hugoniot curve, we also considered a system composed of eight chains of atactic PMMA, where each chain was made up of 45 repeat units (~ 5000 atoms). Again, we observed that the total energy per n and density continued to vary with simulation time, even after 10 ns of equilibration during the NPT simulation under ambient conditions (reference state) (see figure 4).

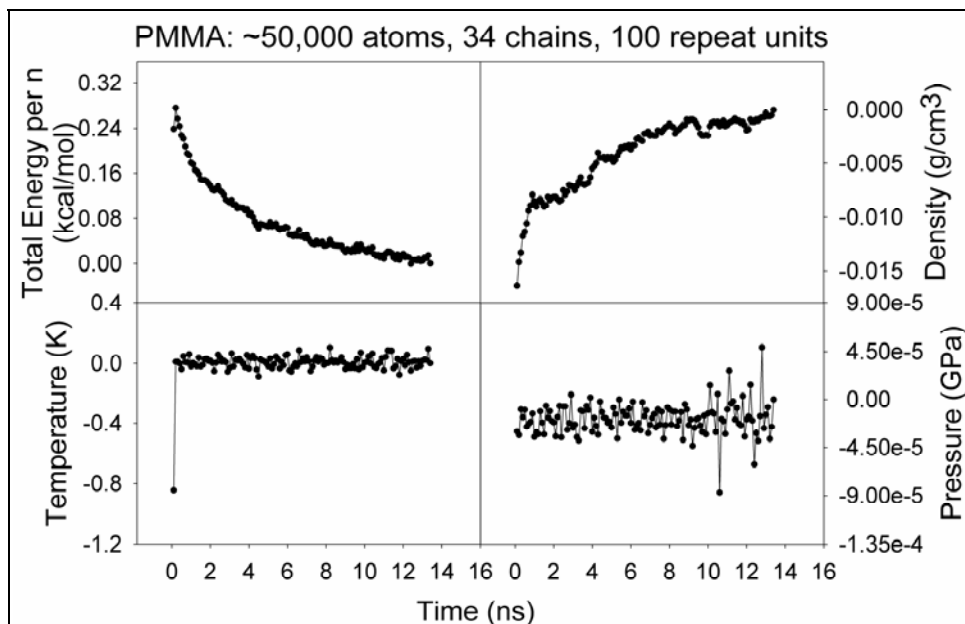


Figure 2. Relative values of the total energy per monomer, density, temperature, and pressure vs. time obtained from NPT simulation for the reference state (~298 K, 1 atm). Relative values were calculated by subtracting the value from the end of the simulation from each data point. Each data point is the average of the last 100 ps.

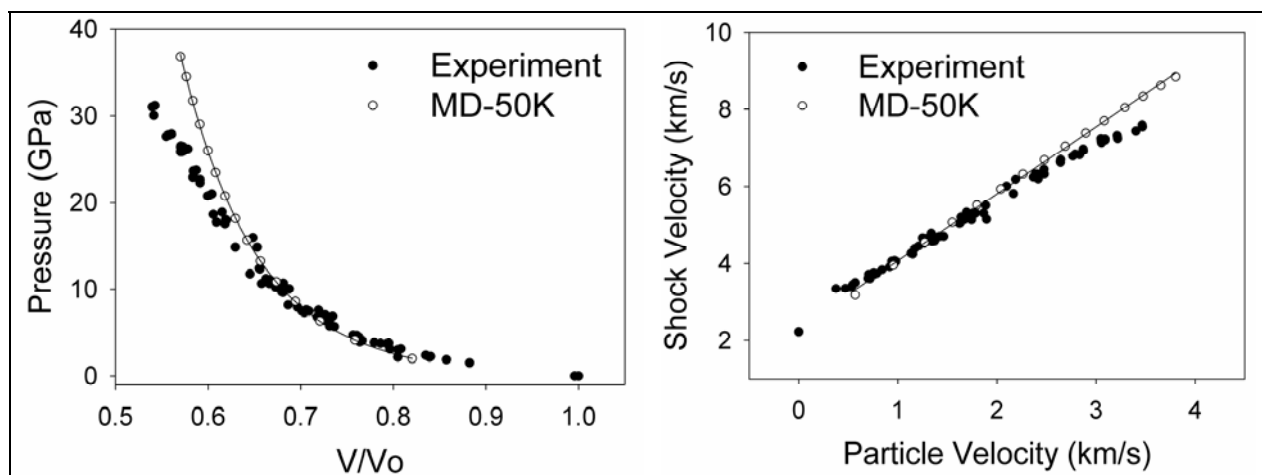


Figure 3. Hugoniot curves for 34 c-100 m-10 ns-0.015 μ s/K-0 compared to experimental values.

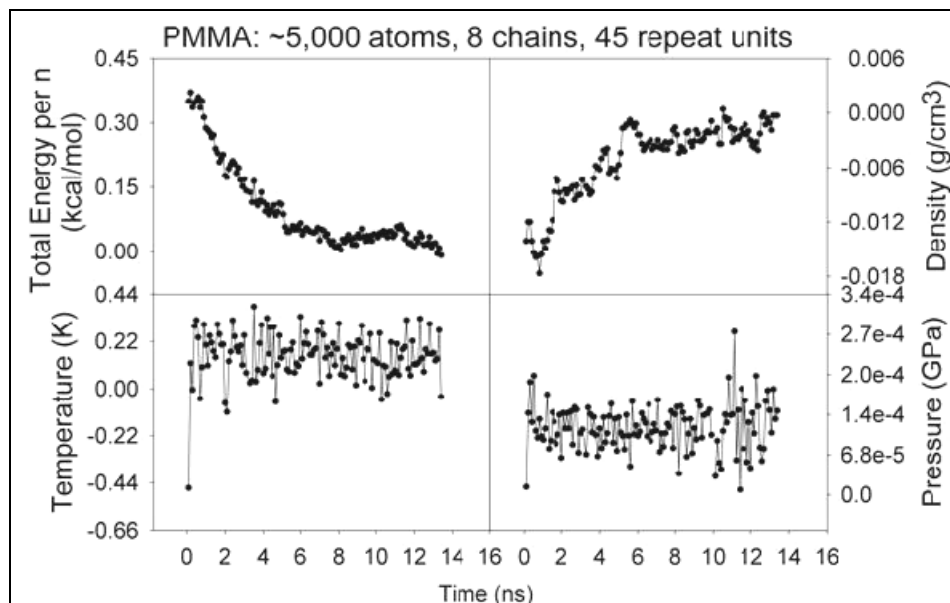


Figure 4. Relative values of the total energy per monomer, density, temperature, and pressure vs. time obtained from NPT simulation for the reference state (~ 298 K, 1 atm). Relative values were calculated by subtracting the value from the end of the simulation from each data point. Each data point is the average of the last 100 ps.

A comparison of the Hugoniot curve for 8 c-45 m-10 ns-0.015 $\mu\text{s/K}$ -0 to 34 c-100 m-10 ns-0.015 $\mu\text{s/K}$ -0 is shown in figure 5. We observed no significant difference between the two simulated curves, indicating that systems composed of shorter and fewer chains (and fewer atoms) were adequate for calculating the Hugoniot curve for PMMA. Using this smaller system, we also performed a study on the effect of NPT equilibration time for the reference state on the Hugoniot curve. Instead of using values after 10 ns of NPT equilibration, we considered values at 2 ns and 100 ps. Hugoniot curves for these two systems are shown in figures 6 and 7, where 8 c-45 m-10 ns-0.015 $\mu\text{s/K}$ -0 did not noticeably vary from 8 c-45 m-2 ns-0.015 $\mu\text{s/K}$ -0 and 8 c-45 m-100 ps-0.005 $\mu\text{s/K}$ -0. From this, we inferred that the calculation was relatively insensitive to the small change in the reference total energy, density, pressure, and temperature achieved by performing the NPT simulation.

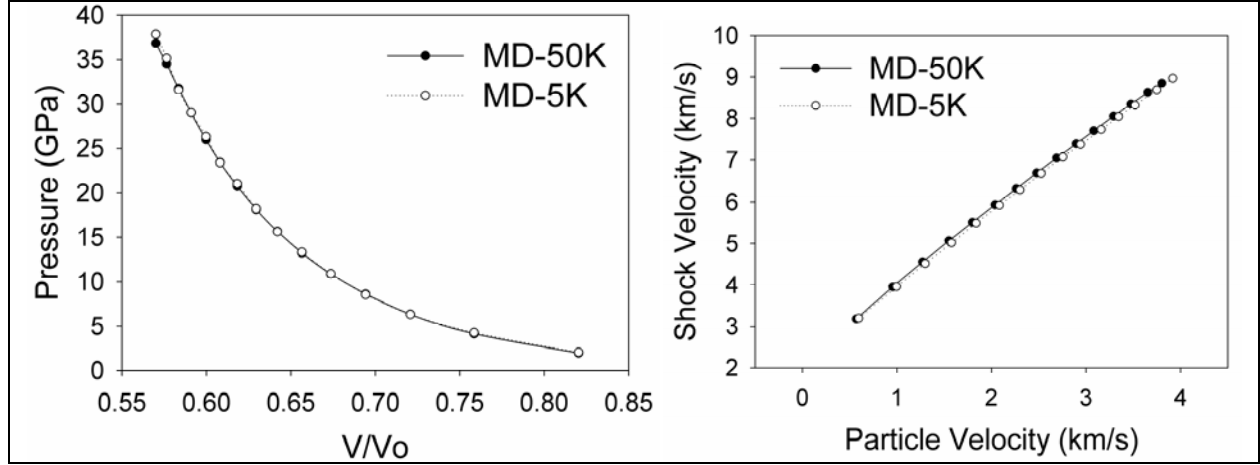


Figure 5. Hugoniot curve for 8 c-45 m-10 ns-0.015 $\mu\text{s/K-0}$ and 34 c-100 m-10 ns-0.015 $\mu\text{s/K-0}$.

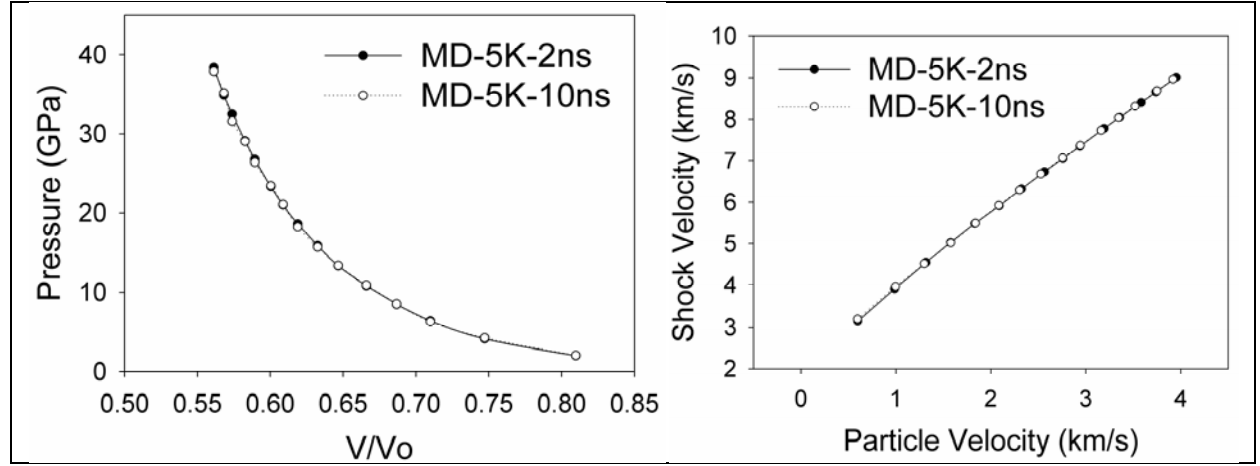


Figure 6. Hugoniot curve for 8 c-45 m-2 ns-0.015 $\mu\text{s/K-0}$ and 8 c-45 m-10 ns-0.015 $\mu\text{s/K-0}$.

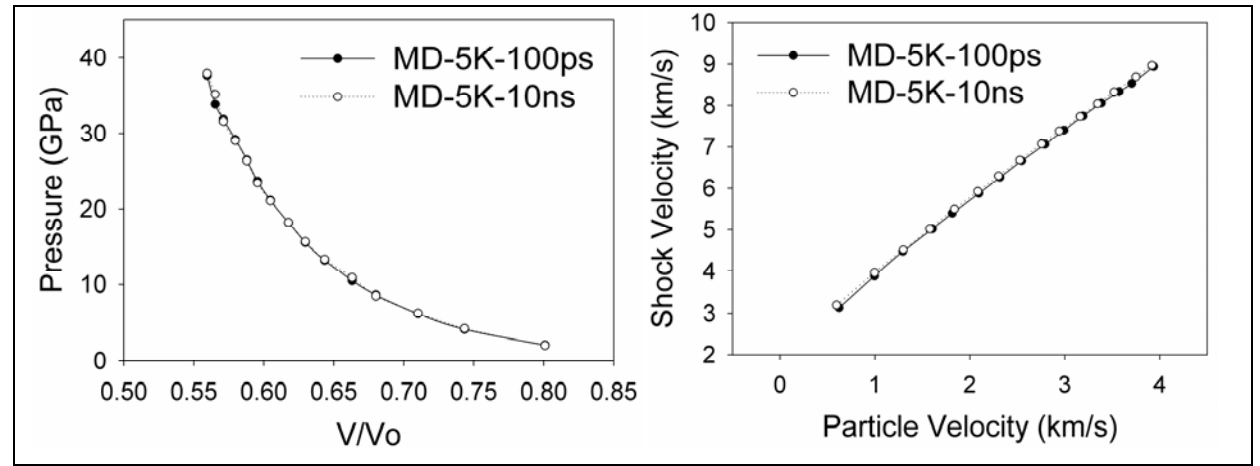


Figure 7. Hugoniot curve for 8 c-45 m-100 ps-0.005 $\mu\text{s/K-0}$ and 8 c-45 m-2 ns-0.015 $\mu\text{s/K-0}$.

To determine whether the method was sensitive to the number of monomers per chain, we considered chains composed of either one (360 c-1 m-100 ps-0.005 $\mu\text{s/K-0}$, ~5000 atoms) or four (33 c-4 m-100 ps-0.005 $\mu\text{s/K-0}$, ~2000 atoms) monomers. The Hugoniot curves for these two simulations are shown in figures 8 and 9. A clear difference between 360 c-1 m-100 ps-0.005 $\mu\text{s/K-0}$ and 8 c-45 m-100 ps-0.005 $\mu\text{s/K-0}$ was shown, indicating that the concept of chain connectivity was important for the Hugoniot calculation. Increasing the chain to four monomers, the calculated Hugoniot curve agreed well with the curve that was produced with a chain composed of 45 monomers.

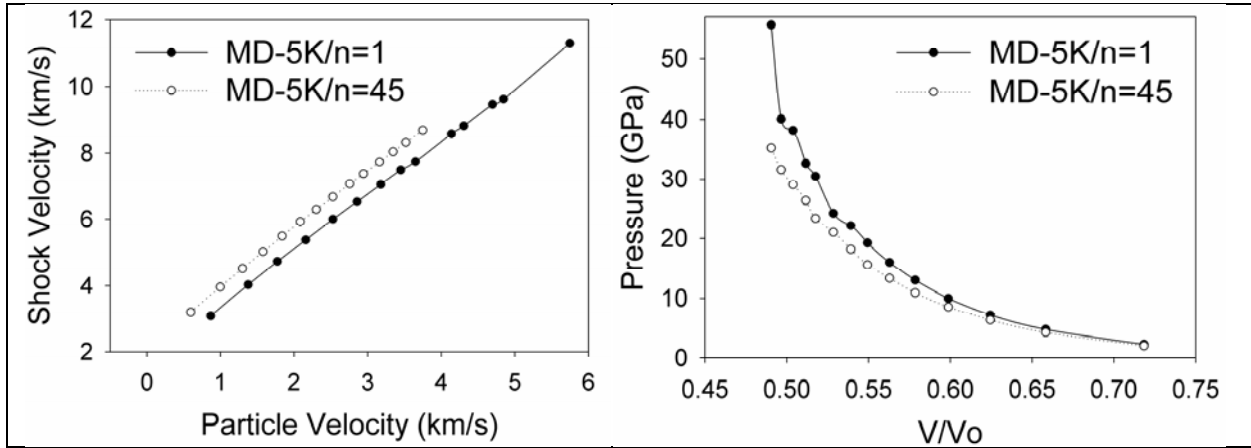


Figure 8. Hugoniot curve for 8 c-45 m-100 ps-0.005 $\mu\text{s/K-0}$ and 360 c-1 m-100 ps-0.005 $\mu\text{s/K-0}$.

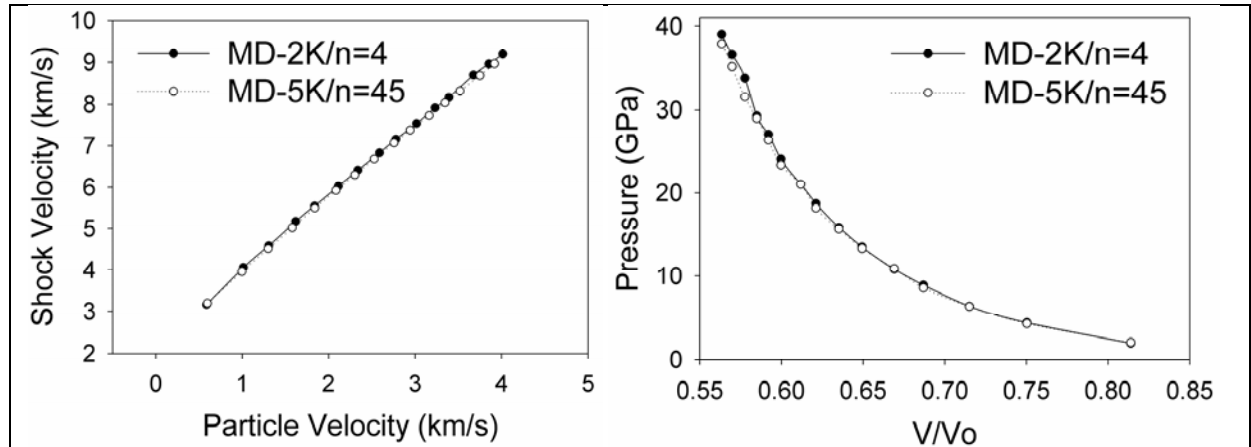


Figure 9. Hugoniot curve for 8 c-45 m-100 ps-0.005 $\mu\text{s/K-0}$ and 33 c-4 m-100 ps-0.005 $\mu\text{s/K-0}$.

This observation allowed us to look towards quantum mechanics to calculate Hugoniot curves. Quantum can be used to look at chain breaking which occurs at high pressures, but this is computationally expensive. As a result, only small systems where the polymers can be represented by a few monomers are computationally feasible.

To determine whether it was necessary to further equilibrate the points around the Hugoniot, which were used to interpolate the Hugoniot temperature and pressure, we performed an additional 10 ns of NVT after the temperature scan. Performing this additional equilibration did decrease the total energy and pressure, as seen in figures 10 and 11, for 34 c-100 m-10 ns-0.015 μ s/K-10 ns and 8 c-45 m-10 ns-0.015 μ s/K-10 ns, respectively. However, it did not decrease significantly where values changed less than $O(1)$, even after an additional 10 ns of equilibration.

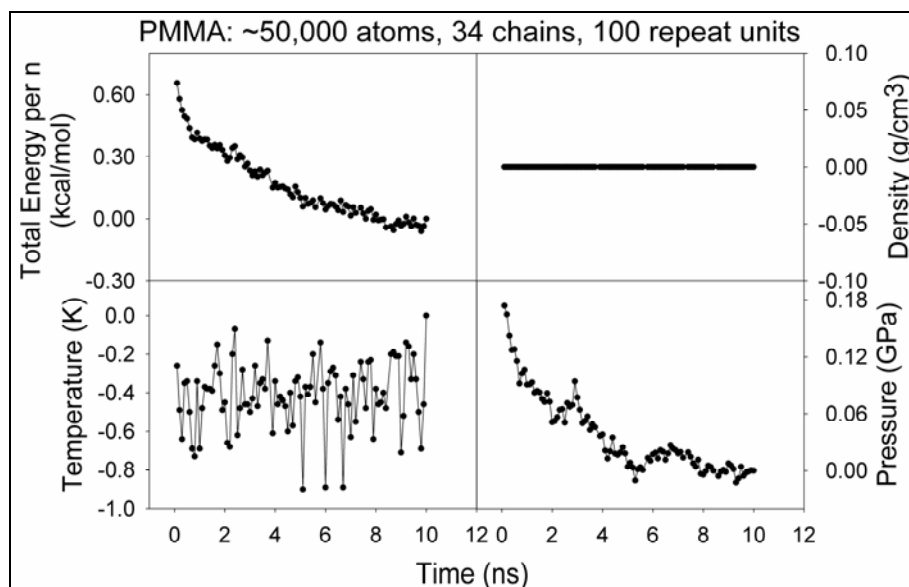


Figure 10. Relative values of the total energy per monomer, density, temperature, and pressure vs. time obtained from NVT simulation at elevated pressure and temperature (~1280 K, 28 GPa). Relative values were calculated by subtracting the value from the end of the simulation from each data point. Each data point is the average of the last 100 ps.

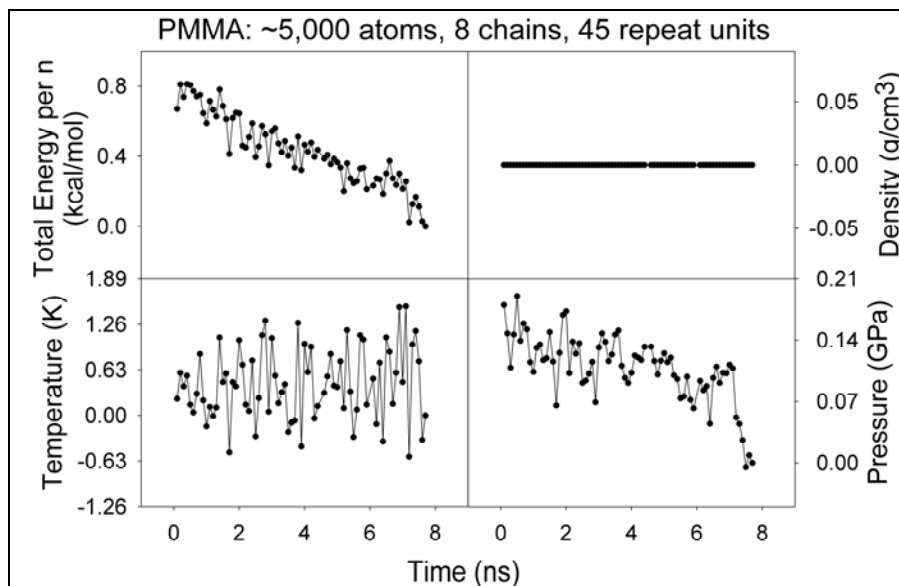


Figure 11. Relative values of the total energy per monomer, density, temperature, and pressure vs. time obtained from NVT simulation at elevated pressure and temperature (~1300 K, 28 GPa). Relative values were calculated by subtracting the value from the end of the simulation from each data point. Each data point is the average of the last 100 ps.

The Hugoniot curves calculated with and without this additional 10-ns NVT equilibration are shown in figures 12 and 13 for 34 c-100 m-10 ns-0.015 $\mu\text{s/K}$ and 8 c-45m-10 ns-0.015 $\mu\text{s/K}$. There were no significant differences between the two curves, thus implying that this additional equilibration was not necessary for PMMA.

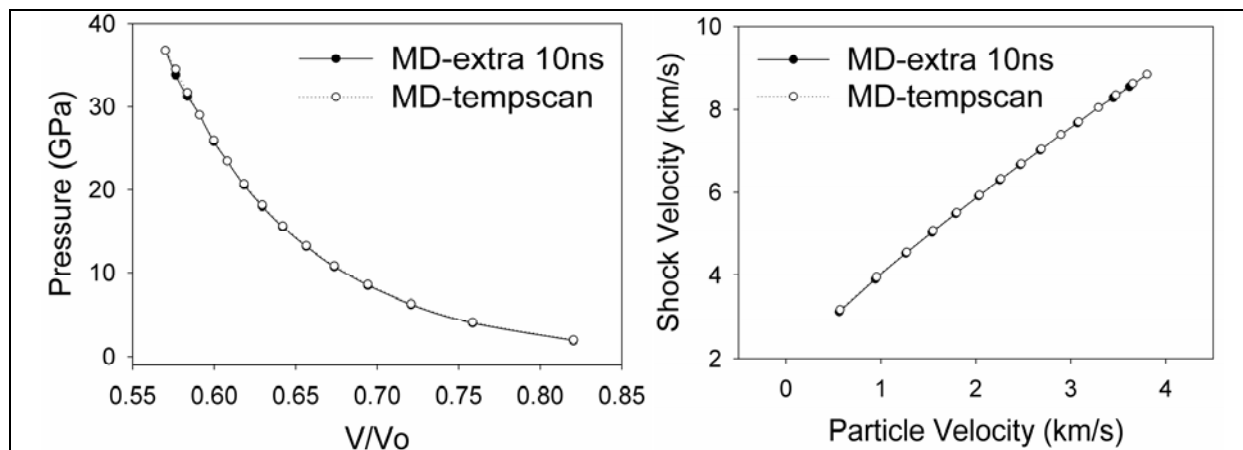


Figure 12. Hugoniot curve for 34 c-100 m-10 ns-0.015 $\mu\text{s/K}$ -10 ns and 34 c-100 m-10 ns-0.015 $\mu\text{s/K}$ -0.

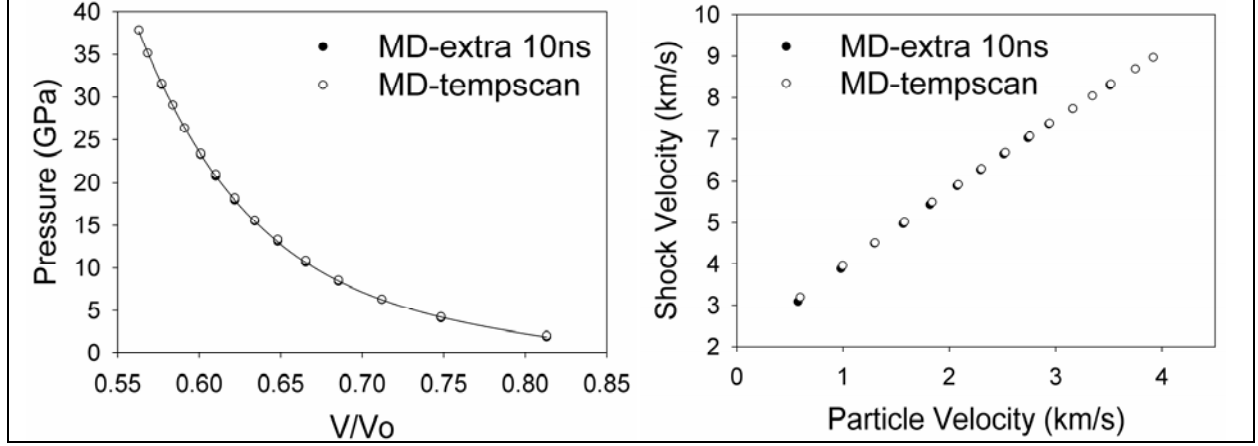


Figure 13. Hugoniot curve for 8 c-45 m-10 ns-0.015 μ s/K-10 ns and 8 c-45 m-10 ns-0.015 μ s/K-0.

5. Conclusion

Through MD simulations implemented through the open source code LAMMPS, PCFF was accessed for predicting PMMA subjected to extreme pressures and temperatures. In addition, we also studied the effect of simulation parameters such as equilibration time, system size, and chain size on the Hugoniot curve. For the former, we found good agreement between the experimental and simulated Hugoniot curves at low and moderate pressures and temperatures. For the latter, we found that the NPT equilibration time for the reference state had a minimal effect on the Hugoniot curve since annealing and relaxing the system adequately optimized the system. In addition, we found that the Hugoniot points could be determined by a quick temperature scan, where further equilibration of the points that bracket the Hugoniot point was unnecessary. Finally, we also found the smaller system sizes were adequate for Hugoniot simulations.

6. References

1. Swanson, D. R.; Mintmire, J. W.; Robertson, D. H.; White, C. T. Detonation Hugoniot From Molecular Dynamics Simulations. *Chemical Physics Reports* **2000**, *18* (10–11), 1871–1881.
2. Erpenbeck, J. J. Molecular Dynamics of Detonation. I. Equation of State and Hugoniot Curve for a Simple Reactive Fluid. *Physical Review A* **1992**, *46*, 6406–6416.
3. Rice, B. M.; Mattson, W.; Grosh, J.; Trevino, S. F. Molecular-Dynamics Study of Detonation. I. A Comparison With Hydrodynamic Predictions. *Physical Review E* **1996**, *53*, 611–622.
4. Maillet, J. B.; Mareschal, M.; Soulard, L.; Ravelo, R.; Lomdahl, P. S.; Germann, T. C.; Holian, B. L. Uniaxial Hugoniot: A Method for Atomistic Simulations of Shocked Materials. *Physical Review E* **2000**, *63*, 016121.
5. Plimpton, S. Fast Parallel Algorithms for Short-Range Molecular Dynamics. *Journal of Computational Physics* **1995**, *117*, 1–19.
6. van Duin, A. C. T.; Dasgupta, S.; Lorant, F.; Goddard, W. A., III. ReaxFF: A Reactive Force Field for Hydrocarbons. *Journal of Physical Chemistry A* **2001**, *105*, 9396–9409.
7. LAMMPS Molecular Dynamics Simulator. <http://lammps.sandia.gov> (accessed November 2011).
8. MAPS interface. <http://www.sciencemoms.com> (accessed November 2011).
9. Accelrys, Inc. *Materials Studio 5.0*; San Diego, CA, 2010.
10. Theodorou, D. N.; Suter, U. W. Detailed Molecular Structure of a Vinyl Polymer Glass. *Macromolecules* **1985**, *18* (7), 1467–1478.

NO. OF
COPIES ORGANIZATION

1 (PDF only)	DEFENSE TECHNICAL INFORMATION CTR DTIC OCA 8725 JOHN J KINGMAN RD STE 0944 FORT BELVOIR VA 22060-6218
1	DIRECTOR US ARMY RESEARCH LAB IMNE ALC HRR 2800 POWDER MILL RD ADELPHI MD 20783-1197
1	DIRECTOR US ARMY RESEARCH LAB RDRL CIO LL 2800 POWDER MILL RD ADELPHI MD 20783-1197
1	DIRECTOR US ARMY RESEARCH LAB RDRL CIO MT 2800 POWDER MILL RD ADELPHI MD 20783-1197
1	DIRECTOR US ARMY RESEARCH LAB RDRL D 2800 POWDER MILL RD ADELPHI MD 20783-1197